IEEE Access
Multidisciplinary ⋮ Rapid Review ⋮ Open Access Journal

Received 24 February 2023, accepted 23 March 2023, date of publication 31 March 2023, date of current version 6 April 2023.

Digital Object Identifier 10.1109/ACCESS.2023.3263473

RESEARCH ARTICLE

Dynamic Modeling and Controller Design for a Parabolic Trough Solar Collector

ANUBHAV GOEL[1], RAJESH MAHADEVA[2], (Member, IEEE), SHASHIKANT P. PATOLE[2], (Member, IEEE), AND GAURAV MANIK[1]

[1]Department of Polymer and Process Engineering, Indian Institute of Technology Roorkee, Roorkee 247667, India
[2]Department of Physics, Khalifa University of Science and Technology, Abu Dhabi, United Arab Emirates

Corresponding authors: Gaurav Manik (gaurav.manik@pe.iitr.ac.in) and Shashikant P. Patole (shashikant.patole@ku.ac.ae)

The work of Anubhav Goel was supported by the Ministry of Human Resource Development (MHRD), India, through the Senior Research Fellowship. This work was supported by the Khalifa University of Science and Technology under the Khalifa University Research Internal Fund.

ABSTRACT The current study unveils an analytical dynamic model of a parabolic trough solar collector (PTSC) and subsequently presents the process to derive the transfer function of the PTSC system. For any PTSC module, output temperature can be related to various operating parameters using the generalized transfer function derivation that has been presented here. Presented model and derivation are applied on a PTSC module tested by Sandia National Laboratory, USA and a transfer function relating the outlet temperature of heat transfer fluid (HTF) with flowrate is derived. PID controller is designed to maintain the HTF outlet temperature by manipulating the flowrate. Natural-inspired algorithms (NIAs), which are uncommon in the context of control systems for PTSCs, are used to tune controllers. Two NIAs, namely Self-adaptive Differential Evolution (SaDE) and African Vultures Optimization Algorithm (AVOA), were used for tuning with minimization of integral of time-weighted absolute error (ITAE) as an objective. It is concluded that SaDE-PID tuned controller outperforms AVOA-PID tuned controller with lower ITAE and other controller characteristics. Also, the designed controller is examined on various grounds as transient response characteristics and performance indexes. This completes the investigation of the integrity of the presented model, process, and controller.

INDEX TERMS African vultures optimization algorithm, controller design, dynamic modeling, parabolic trough solar collector, self-adaptive differential evolution.

I. INTRODUCTION

A. BACKGROUND

It is evident and vital that instead of relying on dwindling fossil fuels, utilization of renewable energy such as solar energy needs to be increased to fulfil the increasing energy requirements. Solar thermal concentrating technologies like parabolic trough solar collectors (PTSCs) which convert solar energy to thermal energy have the ability to greatly assist this notion [1]. PTSC has a parabolic-shaped reflective mirror that focuses solar energy striking its surface onto a heat collector element (HCE) that is located at its focal line. The heat transfer fluid (HTF) travels through the HCE to gain the solar heat which can utilized in different applications [2].

PTSCs can participate as energy source in several fields, such as desalination, industrial activities, and power generation, thereby, making it a relatable option to move towards green energy [3]. Solar energy systems like PTSCs currently face two key drawbacks: solar energy is not always accessible when needed and the associated energy costs are not yet competitive. Control is one of the strategies that has the potential to address these limitations [4]. Therefore, it is essential to conduct studies that can help to increase the effectiveness of control systems related to PTSCs.

B. CHALLENGES

In fossil fuels-based energy systems, the input can be easily manipulated to deliver the desired output. However, in PTSCs the input source (solar irradiation) cannot be changed at will and varies on a daily and seasonal basis, acting as a

The associate editor coordinating the review of this manuscript and approving it for publication was Sudhakar Babu Thanikanti.

disturbance from a control point of view [5]. So, any study that can contribute to the betterment of control systems related to PTSCs would be pivotal. For effective designing of a controller for any system, it is important know about its dynamics [6], [7]. So, it is necessary to develop, an analytical model that can closely capture the dynamics of PTSC.

C. LITERATURE REVIEW

Various studies exploring the possibilities in terms of dynamic modelling, factors to be controlled, factors to be manipulated, and control strategies have been conducted in the past. Few significant ones have been discussed hereafter. Desideri et al. [8] have developed a ThermoCycle (Modelica library) based dynamic model of PTSC. The model was validated for steady-state and transient conditions, by using experimental data from the parabolic trough test loop at the Plataforma Solar de Almería (PSA), Spain. The development and validation of a tool for the dynamic simulation of direct steam generation PTSC loops in conjunction with a control system was conducted by Eck and Hirsch [9]. A dynamic model for PTSC was proposed by Stuetzle et al. [10] and used to develop a model predictive controller for solar electric generating system (SEGS). Both types of sunny days, a summer, and a winter day, are used to test the controller's effectiveness. Additionally, the impact of the control on the plant's gross output is looked at. For a PTSC based collector field for direct steam generation operating in recirculation mode, a work by Guo et al. [11] describes and tests a dynamic model and a generalised predictive control system.

Few studies have laid focus on the tracking control for PTSC. An optimal position control has been pursued by Naidoo and Van Niekerk [12], data is collected from Plataforma Solar de Almeria (PSA) and fed to PLC based software to tune the controller. In a study by Palacios et al. [13], solar tracking controller of PTSC has been designed using traditional PID and then with help of fuzzy logic and particle swarm optimization (PSO). Most of the studies pertaining to the controller design have focused on the control of outlet temperature of HTF. A dead-time compensator and a nonlinear predictive control algorithm were combined by Gálvez-Carrillo et al. [14] to create a Smith Predictor based Nonlinear Extended Prediction Self-Adapting Control method for PTSC based solar field. A PI controller has been designed by Navas et al. [15] to control the oil outlet temperature of a PTSC solar field under the conditions of partial radiation. It was observed that during the days with partial radiation, it is not ideal to run the field at a constant oil output temperature.

A full-scale dynamic model of the ''Andasol II'' PTSCs driven solar thermal power plant is proposed by Al-Maliki et al. [16]. Advanced Process Simulation software was used to create the dynamic model, various parts of the field along with thermal storage were analysed and relevant control circuits designed. A new approach inspired from the functioning of zipper was utilized along with the Lapunov stability analysis was used by Mosbah et al. [17] to design a controller for maintaining the outlet temperature of PTSC. Fuzzy logic-based control strategies were used in few studies, a fuzzy model-based nonlinear model predictive controller was developed earlier by Escaño et al. [18] for a PTSC-based solar facility and to faithfully represent the behaviour of the system dynamics, a fuzzy universal approximate model was introduced by Elmetennani and Laleg-Kirati [19]. To evaluate effective solar radiation and the temperature profiles, an adaptative model predictive control was suggested by Gallego and Camacho [20]. Actual data from the PSA, Spain's ACUREX field were used to validate the control algorithm.

D. RESEARCH GAP AND MOTIVATION

The following key conclusions were drawn after reading the sources mentioned above and other pertinent publications. Firstly, most of the studies have confined to the dynamic modelling and controller design for large PTSC fields like Andasol II or SEGS. Many prevailing studies have their tests and validation revolving around ACUREX field of the PSA, Spain. However, a detailed study confined to the dynamic modeling and control of single PTSC module is still missing. Such a study is essential as it can provide the base that can be extended to various available PTSC module types and can be helpful to aid the energy transition. Further, it is noticed that PID controllers used in process control are frequently designed using nature inspired algorithms (NIAs). However, the utilisation of NIAs in PTSC controller design has not been significant.

E. CONTRIBUTION

Considering the aforementioned deductions, the contribution of this work can be summed up as follows:

- An analytical dynamic model of PTSC has been formulated.
- Method to derive the transfer function for a control system of PTSC has been presented.
- For a PTSC module (LS-2 collector tested by Sandia national laboratory, USA [21]), transfer function relating the HTF outlet temperature with flowrate has been derived.
- Control system for a PTSC module that can maintain the HTF outlet temperature by manipulating the flowrate is investigated through:
  - ❖ Designing of a PID controller
  - ❖ Controller tuning using Self-adaptive Differential Evolution (SaDE) and African Vultures Optimization Algorithm (AVOA).
  - ❖ Testing of the controller for various factors and criteria
  - ❖ Making relevant comparisons to illustrate the best method and conditions.

F. PAPER ORGANIZATION

Section II gives the overview of the PTSC and formulation of its dynamic model. Generic method for the derivation of

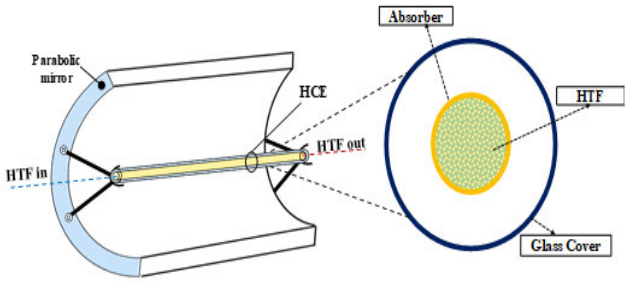

FIGURE 1. Depiction of PTSC along with the cross-sectional view of HCE.

transfer function for the controller of PTSC is covered in Section III. Application of discussed method over a specific PTSC module, controller design, tuning and testing have all been detailed in Section IV. The key findings of this work are outlined in Section VI.

II. DYNAMIC MODELING

A good analytical model that can realize the dynamics of the system is an asset to design a controller. With this aim a detailed analytical dynamic model of PTSC is presented in this section. The illustration in Figure 1 shows the various parts of PTSC and also illustrates a cross sectional view of HCE for better understanding of impending analysis.

The PTSC is a type of line-focusing collector that concentrates solar energy and transforms it into useful heat energy. It has a reflective mirror with a parabolic form that converges solar energy striking its surface to the heat collecting element (HCE) positioned at its focal line. The HCE is made up of the metal absorber pipe through which the heat transfer fluid (HTF) passes. An absorber is enclosed in a glass envelope and the annulus between them is vacuumed. Also, a solar selective absorber coating (SSAC) is applied on the absorber to increase solar absorption. By considering the energy balances across the HCE surfaces, the dynamics of the PTSC can be investigated by using the following set of equations [2], [5]:

$$\rho_f C_{p_f} A_f \frac{\partial T_f}{\partial t}(t,x) + \rho_f C_{p_f} V_f \frac{\partial T_f}{\partial x}(t,x) = \pi D_{a_i} h_f \left(T_{ab}(t,x) - T_f(t,x)\right) \tag{1}$$

$$\rho_{ab} C_{p_{ab}} A_{ab} \frac{\partial T_{ab}}{\partial t}(t,x) = \eta_O I_O w - \pi D_{a_i} h_f \left(T_{ab}(t,x) - T_f(t,x)\right) - \pi D_{a_o} H_l \left(T_{ab}(t,x) - T_{su}(t)\right) \tag{2}$$

Few of the essential parameters and model variables from above equations are summed up in Table 1. Details about the remaining and their estimations are discussed thereafter.

Now, h_f represents the represents the convective heat transfer coefficient (W/m°C) for heat transfer between absorber and pipe, and can be computed as:

$$h_f = Nu_{D_{a_i}} \frac{k_f}{D_{a_i}} \tag{3}$$

TABLE 1. Parameters and model variables.

Parameter	Interpretation	SI unit
ρ_f	Density of HTF	kg/m^3
C_{p_f}	Specific heat capacity of HTF	J/kg°C
A_f	Cross-sectional area for HTF flow	m^2
ρ_{ab}	Density of metallic absorber pipe	kg/m^3
A_{ab}	Cross-sectional area of the absorber pipe wall	m^2
$C_{p_{ab}}$	Specific heat capacity of metallic absorber pipe	J/kg°C
T_f	Mean HTF temperature	°C
V_f	Volumetric flow rate of HTF	m^3/s
D_{a_i}	Inside diameter of the absorber	m
w	Width of the parabolic trough	m
T_{ab}	Mean absorber temperature	°C
T_{su}	Surroundings temperature	°C
I_O	direct normal irradiation (DNI) per unit length of collector	W/m^2

Here, $Nu_{D_{a_i}}$ represents the Nusselt number based on D_{a_i} and K_f is the thermal conductivity of HTF.

It is evident that convective heat transfer relies on the flow regime, for the PTSC, if Reynolds number (Re) is $Re < 2300$ i.e. HTF flow is laminar then $Nu_{D_{a_i}} = 4.36$ [22]. Though under operation the HTF flow is normally turbulent and for this condition $Nu_{D_{a_i}}$ can be estimated by the correlation given by Gnielinski [23]:

$$Nu_{D_{a_i}} = \frac{\frac{fr}{8\left(Re_{D_{a_i}} - 1000\right)Pr_f}}{1 + 12.7\sqrt{fr}/8\left(Pr_f^{2/3} - 1\right)} \left(\frac{Pr_f}{Pr_{a_i}}\right)^{0.11} \tag{4}$$

where, Pr_{a_i} and Pr_f are Prandtl numbers calculated at respective temperatures and $Re_{D_{a_i}}$ is the Reynolds number. Furthermore, fr is the friction factor at the absorber's inner surface, which may be determined using Colebrook's correlation [24]:

$$fr = \left[1.5635\, ln\left(Re_{D_{a_i}}/7\right)\right]^{-2} \tag{5}$$

In equation (2), H_l depicts the heat loss coefficient which can be used to represent all of HCE's heat losses [25] and given as:

$$H_l = \left[\frac{A_{a_o}}{\left(h_{g_o - sky\,Rad} + h_{g0-s}\right)A_{g_o}} + \frac{1}{h_{a_o - g_i} + h_{a_o - g_i\,Rad}}\right]^{-1} \tag{6}$$

Here, A_{a_o} and A_{g_o} are the area of outer surface of absorber and of the glass cover, h_{g0-s}, $h_{a_o-g_i}$ are heat loss coefficients for the convective heat loss occurring from HCE to surrounding and in annulus space respectively. While, $h_{g_o-sky\,Rad}$ and $h_{a_o-g_i\,Rad}$ are heat loss coefficients for the radiative heat losses to ambient and in annulus. All these coefficients are estimated with help of correlations described hereinafter.

Firstly, $h_{a_o-g_i}$ is calculated with annulus region considered to be evacuated (Annulus pressure $<$ 0.013 Pa). Heat is transferred *via* molecular conduction at this pressure and can be estimated using the correlation given by Ratzel et al. [26].

$$h_{a_o-g_i} = \frac{k_{ga}}{\frac{D_{ao}}{ln\left(\frac{D_{g_i}}{D_{ao}}\right)} + b\lambda\left(\frac{D_{ao}}{D_{g_i}}+1\right)} \quad \text{where,}$$
$$b = \frac{(2-A)\,(9\gamma-5)}{2A\,(\gamma+1)} \quad \text{and } \lambda = \frac{2.331\times10^{-20}(T_{a_o-g_i})}{(P_a\delta^2)} \tag{7}$$

where, k_{ga} is thermal conductivity of annulus gas, D_{g_i} is inside diameter of the glass cover, b is the interaction coefficient, λ is ratio of mean free path between collisions of molecules, P_a is the annulus gas pressure, $T_{a_o-g_i}$ is the average annulus temperature calculated at $\left(T_{a_0}+T_{g_i}\right)/2$, and δ is the molecular diameter of annulus gas.

Then, h_{g_0-s} is evaluated as:

$$h_{g_0-s} = \frac{k_{air}}{D_{g_0}} Nu_{D_{g_0}} \tag{8}$$

Here, k_{air} is the thermal conductivity of air and $Nu_{D_{g_0}}$ is the Nusselt number evaluated at D_{g_0}. For estimation of $Nu_{D_{g_0}}$, a method considering a mixed convection regime is used [27]. Initially, the Nusselt number is determined for natural convection (Nu_N) [28], [29].

$$Nu_N = \left[(Nu_l)^{10} + (Nu_t)^{10}\right]^{1/10} \tag{9}$$

Such that $Nu_l = \frac{2\mathcal{F}}{\ln\left(1+2\mathcal{F}/Nu^T\right)}$, *where* $Nu^T = 0.772C_yRa_{air}^{1/4}$ and $\mathcal{F} = 1 - \frac{0.13}{(Nu^T)^{0.16}}$

$$Nu_t = C_xRa_{air}^{1/3}$$

where, $C_x = 0.103$ and $C_y = 1.6$ are constants, Ra_{air} is the Rayleigh number based on surrounding air, Nu_l is the Nusselt number for laminar, while Nu_t is for turbulent heat transfer from glass cover.

Next, the Nusselt number is determined for forced convection (Nu_F).

$$Nu_F = \mathcal{U}Re_{air}^{\mathcal{V}} \tag{10}$$

where, Re_{air} denotes the Reynolds number calculated from ambient air characteristics and $\mathcal{U}$, $\mathcal{V}$ are constants that can be utilized as given in [30].

Afterwards, an equivalent Reynolds number (Re^{δ}) is calculated by applying the relation $Nu_N = Nu_F$, as reported by [30] and [31], to incorporate both convection mechanisms.

$$Re^{\delta} = [Nu_N/\mathcal{U}]^{1/\mathcal{V}} \tag{11}$$

The blended flow's total Reynold's number (Re_{eff}) is then computed as:

$$Re_{eff} = \left[\left(Re^{\delta}\right)^2 + (Re_{air})^2 + 2Re_{air}Re^{\delta}\cos\phi\right]^{1/2} \tag{12}$$

By substituting Re_{air} for Re_{eff} in equation (10) the $Nu_{D_{g_0}}$ is obtained, and the relationship is modified as:

$$Nu_{D_{g_0}} = \mathcal{U}Re_{eff}^{\mathcal{V}} \tag{13}$$

To estimated radiative heat transfer coefficients, $h_{g_o-sky\,Rad}$ and $h_{a_o-g_i\,Rad}$ are expressed analogously to h_{g_0-s} and $h_{a_o-g_i}$ and can be computed as:

$$h_{a_o-g_i\,Rad} = \frac{\sigma\left(T_{a_o}^2+T_{g_i}^2\right)\left(T_{a_o}+T_{g_i}\right)}{\frac{1}{\varepsilon_{a_o}}+\frac{A_{abs}}{A_g}\left(\frac{1}{\varepsilon_g}-1\right)} \tag{14}$$

$$h_{g_o-sky\,Rad} = \varepsilon_g\sigma\left(T_{g_o}+T_{sky}\right)\left(T_{g_o}^2+T_{sky}^2\right) \tag{15}$$

where, $F_{a_oe_i}$ is view factor, T_{sky} is the temperature of the sky, ε_{a_o} is the emissivity of SSAC, σ is Stefan-Boltzmann constant, ε_g is the emissivity of glass cover, and A_g is area of outside surface of glass cover.

Another factor is η_O which is known as optical efficiency, it reflects the percentage of solar energy that the absorber is capable of absorbing and can be expressed as [25]:

$$\eta_O = \Upsilon T_{ge}\rho_m\alpha_{ab}K_\theta\,\epsilon_{el}\epsilon_{sh} \tag{16}$$

Herein, ρ_m is mirror reflectivity, α_{ab} is absorptance of the absorber, and T_{ge} is transmittance of the glass envelope. Υ represents an intercept factor accounted as $\Upsilon = \xi_g\xi_t\xi_{dm}\xi_{dhc}\xi_m$. Various factors that are considered for its estimation are imperfections in solar tracking system (ξ_{st}), dirt on mirror (ξ_{dm}) aand heat collector (ξ_{dhc}), misalignment between heat collector and mirror (ξ_{ia}), and other unaccounted errors (ξ_u). K_θ is incidence angle modifier and is a statistical relationship generated from experimental data for a specific collector. ϵ_{el} is end loss effect that sums up the loss occurring due to the improper irradiations at the ends of HCE and expressed as [32]:

$$\epsilon_{el} = 1 - \frac{f_{rc}}{l_{rc}}\tan\theta \tag{17}$$

Here, l_{rc} is the length and f_{rc} is focal length of the collector.

ϵ_{sh} is shading loss that represents the loss occurring due to the underutilization of mirror surface caused by the shadows of HCE and support brackets. The following correlation can be used to approximate this loss:

$$\epsilon_{sh} = 1 - \frac{D_{a_o}}{l_{rc}}tan\,\theta \tag{18}$$

III. DERIVATION OF TRANSFER FUNCTION

It is evident that for designing or tuning a controller for PTSC, a transfer function that relates the output and manipulated variable is required. To obtain that, relevant operations are performed on equations (1) and (2) which are discussed now.

It can be ascertained from equations (3) and (18) that equations (1) and (2) comprises several non-linear terms. So, primarily, to get at linear approximations of the non-linear

elements simplification and Taylor series expansions are performed as follows [33]:

$$\frac{\partial T_f}{\partial t} = -(v - v_s)\frac{\partial T_{f_s}}{\partial x} - v_s\frac{\partial T_f}{\partial x} + \frac{1}{\tau_1}\left(T_{ab} - T_f\right) \quad (19)$$

$$\frac{\partial T_{ab}}{\partial t} = I_O\Psi - \frac{1}{\tau_2}\left(T_{ab} - T_{su}\right) - \frac{1}{\tau_{12}}\left(T_{ab} - T_f\right) \quad (20)$$

Here, $\Psi = \frac{\eta_O w \alpha_{ab}}{\rho_{ab} C_{p_{ab}} A_{ab}}$, $\tau_1 = \frac{\rho_f C_{pf} A_f}{\pi D_{a_i} h_f}$, $\tau_2 = \frac{\rho_{ab} C_{p_{ab}} A_{ab}}{\pi D_{a_i} h_f}$, $\tau_{12} = \frac{\rho_{ab} C_{p_{ab}} A_{ab}}{\pi D_{a_o} H_l}$ and subscript s is representing steady state value.

The deviation terms ($\widetilde{T_{ab}} = T_{ab} - T_{ab_s}$, $\widetilde{I_O} = I_o - I_{o_s}$, $\widetilde{T_f} = T_f - T_{f_s}$, and $\widetilde{v} = v - v_s$) are then incorporated around the following steady state conditions:

$$0 = -v_s\frac{\partial T_{f_s}}{\partial x} + \frac{1}{\tau_1}\left(T_{ab_s} - T_{f_s}\right) \quad (21)$$

$$0 = I_{o_s}\Psi - \frac{1}{\tau_2}\left(T_{ab_s} - T_{su_s}\right) - \frac{1}{\tau_{12}}\left(T_{ab_s} - T_{f_s}\right) \quad (22)$$

Subsequently, equation (21) is subtracted from (19) and equation (22) is subtracted from (20) to get the following partial differential equations.

$$\frac{\partial \widetilde{T_f}}{\partial t} = -\widetilde{v}\frac{dT_{f_s}}{dx} - v_s\frac{\partial \widetilde{T_f}}{\partial x} + \frac{1}{\tau_1}\left(\widetilde{T_{ab}} - \widetilde{T_f}\right) \quad (23)$$

$$\frac{\partial \widetilde{T_{ab}}}{\partial t} = \widetilde{I_O}\Psi - \frac{1}{\tau_2}\left(\widetilde{T_{ab}} - \widetilde{T_{su}}\right) - \frac{1}{\tau_{12}}\left(\widetilde{T_{ab}} - \widetilde{T_f}\right) \quad (24)$$

To proceed further for the derivation of transfer function, Laplace transform is applied on equations (23) and (24).

$$s\widetilde{T_f}(s) = -\widetilde{v}(s)\frac{dT_{f_s}}{dx} - v_s\frac{d\widetilde{T_f}(s)}{dx} + \frac{1}{\tau_1}\left(\widetilde{T_{ab}}(s) - \widetilde{T_f}(s)\right) \quad (25)$$

$$s\widetilde{T_{ab}}(s) = \widetilde{I_O}(s)\Psi - \frac{1}{\tau_2}\left(\widetilde{T_{ab}}(s) - \widetilde{T_{su}}(s)\right) - \frac{1}{\tau_{12}}\left(\widetilde{T_{ab}}(s) - \widetilde{T_f}(s)\right) \quad (26)$$

Equations (25) and (26) are then restructured to eliminate $\widetilde{T_{ab}}(s)$ and get single equation in terms of $\widetilde{T_f}(s)$.

$$\frac{d\widetilde{T_f}(s)}{dx} + \frac{a(s)}{v_s}\widetilde{T_f}(s) = -\frac{\widetilde{v}(s)}{v_s}\frac{dT_{f_s}}{dx} - \frac{\tau_2 b(s)\Psi}{v_s}\widetilde{I_O}(s) + \frac{b(s)}{v_s}\widetilde{T_a}(s) \quad (27)$$

where, $a(s) = S + \frac{1}{\tau_1} - \frac{\tau_2}{\tau_1(\tau_2\tau_{12}s+\tau_2+\tau_{12})}$ and $b(s) = \frac{\tau_{12}}{\tau_1(\tau_2\tau_{12}s+\tau_2+\tau_{12})}$

To obtain a generic equation that can relate the output of PTSC (outlet HTF temperature) with other variables like HTF flow rate, solar irradiation, and others, equation (27) is further solved with boundary condition $\widetilde{T_f}(s,x) = \widetilde{T_f}(s,0)$ at $x = 0$ and following equation is established [34].

$$\widetilde{T_f}(s) = -\widetilde{v}(s)\frac{T_{a_s} + I_s\tau_2\Psi - T_{f_{so}}}{a(s)c - v_s}\left[e^{-\frac{x}{c}} - e^{-\frac{a(s)}{v_s}x}\right] + \widetilde{I_O}(s)\tau_2\Psi\frac{b(s)}{a(s)}\left[1 - e^{-\frac{a(s)}{v_s}x}\right] + \widetilde{T_{ab}}(s)\frac{b(s)}{a(s)}\left[1 - e^{-\frac{a(s)}{v_s}x}\right] + \widetilde{T_f}(s,0)e^{-\frac{a(s)}{v_s}x} \quad (28)$$

This equation can be used to derive the transfer function between HTF outlet temperature and manipulated variables, as the purpose of this investigation is to ensure control of HTF flow rate for maintaining outlet temperature. A single input single output (SISO) transfer function is obtained by considering all variables except HTF velocity to be at steady state. For this, equation (28) is extended for $x = l_{rc}$ and then simplified as:

$$\frac{\widetilde{T_f}(s,L)}{\widetilde{v}(s)} = -\frac{T_{a_s} + I_s\tau_2\Psi - T_{f_{so}}}{c}e^{-\frac{x}{c}}\frac{s + \frac{\tau_{12}+\tau_2}{\tau_{12}\tau_2}}{s^2 + \left(\frac{\tau_{12}+\tau_2}{\tau_{12}\tau_2} + \frac{\tau_2}{\tau_1(\tau_{12}+\tau_2)}\right)s} \times \underbrace{\left[1 - e^{-\frac{l_{rc}}{v_s}\left(s + \frac{\tau_2}{\tau_1(\tau_{12}+\tau_2)}\left(\frac{s}{s+\frac{\tau_1^2+\tau_2}{\tau_1^2+\tau_2}}\right)\right)}\right]}_{R(s)} \quad (29)$$

Here, $c = v_s\tau_1(1 + \frac{\tau_2}{\tau_{12}})$.

It is to be noted that this equation has a term $R(s)$ having a complex expression in s-domain. This term represents the transfer function that models the resonance mode of system while the remaining part represent the low order transfer function of the system. As the purpose of the study is to capture the dynamics of the system and to test/suggest a relevant control schemes, so in line with suggestion by Camacho et al. [35], [36] equation (29) needs to be approximated to a standard form and then term $R(s)$ can be overlooked. The resultant equation is shown below.

$$G(s) = \frac{\widetilde{T_f}(s,L)}{\widetilde{q}(s)} = K_a\frac{-\beta_a s + 1}{s(\tau_a s + 1)}e^{-t_d s} \times \underbrace{\left[1 - e^{-t_r s}\left(\frac{-\beta s + 1}{\tau s + 1}\right)\right]}_{R(s)} \quad (30)$$

The remaining transfer function can capture the key system dynamics and the impact of disturbances such that it can assist to design high-performance control systems. Thus, the transfer function relating the outlet HTF temperature with HTF flow rate is given as:

$$\frac{\widetilde{T_f}(s,L)}{\widetilde{q}(s)} = K_a\frac{-\beta_a s + 1}{s(\tau_a s + 1)}e^{-t_d s} \quad (31)$$

where, $K_a = -\frac{1}{A_f}\frac{T_{a_s}+I_s\tau_2\Psi-T_{f_{so}}}{c}e^{-\frac{x}{c}}\frac{\tau_1(\tau_{12}+\tau_2)^2}{\tau_1(\tau_{12}+\tau_2)^2+\tau_{12}\tau_2^2}$, $\beta_a = -\frac{\tau_{12}\tau_2}{\tau_{12}+\tau_2}$, and $\tau_a = \frac{\tau_1\tau_2\tau_{12}(\tau_{12}+\tau_2)}{\tau_1(\tau_{12}+\tau_2)^2+\tau_{12}\tau_2^2}$.

TABLE 2. Geometrical parameters for LS-2 collector [21].

Specifications	Value
Collector length, l_{cl}	7.8 m
Collector width, w_{cl}	5 m
Inner diameter of absorber, D_{a_i}	0.066 m
Outer diameter of absorber, D_{a_o}	0.070 m
Inner diameter of glass envelope, D_{e_i}	0.109 m
Outer diameter of glass envelope, D_{e_o}	0.115 m
Length of HCE, l_{hce}	8 m
Focal length of collector, f_{rc}	1.84 m
Collector aperture area, A_{cl}	39.2 m^2

Furthermore, the transfer function in equation (31) is approximated to derive first order model for system control. The first order transfer function for process control is generally given as:

$$\frac{\widetilde{T}_f(s,L)}{\widetilde{q}(s)} = \frac{K}{(\tau s+1)} e^{-t_d s} \tag{32}$$

Here, K represents the system gain which can be estimated as per the deductions made by Cirre et al. [37], thus, computed as:

$$\lim_{s\to 0} G(s) = K_a(t_r + \beta + \tau) \tag{33}$$

τ is the time constant of the system and t_d depicts the time delay (dead time) that occurs due to the position of temperature sensor. For instance, based on the current measurement a controller may change the HTF flowrate, but it will be sensed only after some time by the sensor placed at the outlet of HCE. This is not fixed but is inversely proportional to the HTF velocity and can be estimated as $t_d = l_{rc}/v$ [38].

IV. TRANSFER FUNCTION FOR PTSC MODULE

The method presented for the derivation of transfer function is applied on a PTSC module tested by Sandia National Laboratories (SNL), USA [21]. Various performance tests have been conducted by SNL on a PTSC module named as LS-2 and mentioned to be used in Solar Electric Generating System (SEGS). Geometric parameters required for estimation of transfer function are gathered for LS-2 collector and summarized in Table 2.

As discussed in Section III, the derivation of transfer function is facilitated by the Taylor series expansion around a steady state of the system. Hence, the required steady state values are considered here are from a specific set of operating conditions captured from the test report published by SNL for above mentioned LS-2 collector. The operating conditions under which the PTSC is examined are DNI (W/m^2) = 968.2, Wind (m/s) = 3.70, Flow rate (L/min) = 47.80, T_{amb} (°C) = 22.4, T_{in} (°C) = 151.00, Outlet Temperature (°C) = 173.30, Efficiency = 70.90%.

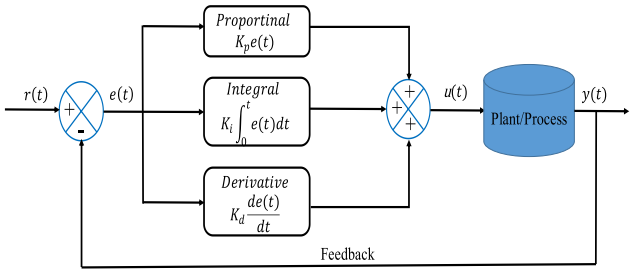

FIGURE 2. A schematic of PID controller.

Besides, the geometric parameters and operating conditions, values for heat transfer coefficients, optical efficiency, etc. are also required for the transfer function estimation. For this, the correlations described in Section II are used, though to estimate them temperature values at different surfaces of HCE is a prerequisite. Thus, a thoroughly validated thermal model of PTSC proposed by [39] that can be used to determine the temperature profile of HCE in radial direction is exploited in conjunction.

With the help of preceding discussion and method presented in Section III, the first order transfer function relating the output temperature with HTF flowrate for a PTSC module is as:

$$G_p(s) = \frac{\widetilde{T}_f(s,L)}{\widetilde{q}(s)} = \frac{-866.9}{(313.2s+1)} e^{-33.5s} \tag{34}$$

V. CONTROLLER DESIGN

It is widely known that Proportional, Integral, and Derivative (PID) control loops account for about 90% of process control loops. Also, the primary challenge encountered by them is the precise tuning of their parameters [40], [41]. The usage of PID controllers is appealing to process industries owing to its simplicity, ease of implementation, and resilience [42]. The desired closed-loop system performance can be attained by adjusting the controller parameters, referred as controller tuning. The controller parameters for PID control signifies the gains for proportional (P), integral (I), and derivative (D) controllers. A better conception of the same can be attained by looking at Figure 2 that shows the block diagram of a PID controller.

The mathematical description of PID controller can be given as:

$$G_{PID}(t) = K_p e(t) + K_i \int_0^t e(t)\,dt + K_d \frac{de(t)}{dt} \quad \text{(time domain)} \tag{35}$$

$$G_{PID}(s) = K_p E(s) + K_i \frac{E(s)}{s} + K_d s E(s) \quad \text{(s-domain)} \tag{36}$$

where, K_p, K_i, and K_d are proportional gain, integral gain, and derivative gain respectively. $e(t)$ represents the value of error estimated by subtracting the actual system output ($y(t)$)

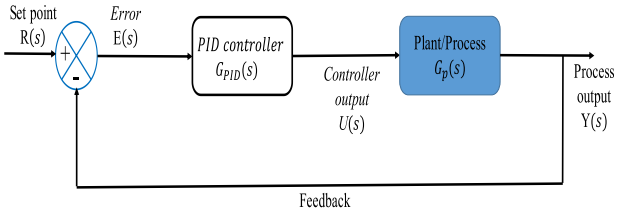

FIGURE 3. Control loop for PTSC with PID controller.

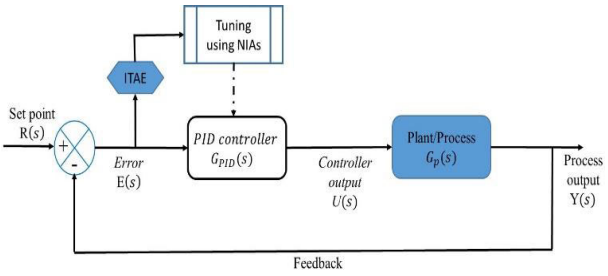

FIGURE 4. Illustration of nature inspired algorithm (NIA) controller for PTSC to emphasize the tuning objective.

from reference value ($r(t)$), such that $e(t) = r(t) - y(t)$ [43]. Based on this error, PID controller varies the values of K_p, K_i, and K_d to minimize $e(t)$.

In the current study, focus is to design a controller for PTSC such that a specific output temperature can be maintained by varying the HTF flowrate. Temperature control is quite important for industries because if temperatures are permitted to fluctuate too much, they can interfere with the production process in addition to destroying the final product. A process transfer function [$G_p(s)$] relating the output temperature with HTF flowrate is derived and shown in equation (34). Subsequently, a PID controller depicting the control loop for required control in context of PTSC is proposed as illustrated in Figure 3.

VI. OBJECTIVE FUNCTION FORMULATION

As highlighted earlier, precise tuning of PID parameters is a challenging task. Many a times the tuning is performed by hit and trial to reach an acceptable error value. Though, in process control where system is online continuously and a minute error can lead to an undesirable operation or even a shutdown of a system, it is important to have an automated method to tune the controller. To design such a controller, firstly, we must have some understanding of what we desire as an ideal response before we can be satisfied with the response of a control system for a set of control parameters. Secondly, a criterion is required that reduces the complete response to a single figure of merit, such that different responses obtained *via* use of distinct sets of controller parameters can be easily compared [44]. As illustrated in Figure 4, one such criterion is integral of time-weighted absolute error (ITAE) which is being utilized here as an objective function to tune the controller for PTSC.

Tuning a PID controller is a complex problem and often the nature inspired algorithms (NIAs) such as particle swarm optimization (PSO), genetic algorithm (GA), and others are required for it [45], [46]. Thus, representing a controller tuning as an optimization problem with a defined objective function becomes important to ease and streamline the implementation of NIAs. In this study, the objective of the tuning of controller parameters is thus expressed through the minimization of ITAE and can be mathematically represented as:

$$\begin{aligned} &Minimize \left[F_{ITAE} = \int_0^\infty |e(t)|\, tdt \right] \\ &\text{Subjected to: } K_{p_{min}} \le K_p \le K_{p_{max}}, \quad K_{i_{min}} \le K_i \le K_{i_{max}}, \\ &\qquad \text{and } K_{d_{min}} \le K_d \le K_{d_{max}} \end{aligned} \tag{37}$$

where, F_{ITAE} is the objective function, K_p, K_i, and K_d are the gains of the PID controller to control HTF flowrate of a PTSC.

VII. CONTROLLER TUNING USING NIAs

Metaheuristic algorithms or simply NIAs are often used for designing of PID controller used in industrial process control [47], [48], [49]. Still, the use of NIAs in controller design for PTSCs is relatively unnoticeable and this study explores the possibilities in this context. The tuning of controller designed for PTSC is attempted *via* two different algorithms namely Self-adaptive Differential Evolution (SaDE) and African Vultures Optimization Algorithm (AVOA). For a fundamental understanding, Figure 5 depicts a broader view of the optimization process followed here.

In Section 4.3, how a controller tuning problem can be formulated as an optimization problem is explained. Figure 5 shows how to apply NIAs to solve this optimization problem and presents the Simulink model developed to determine the resultant ITAE at given values of K_p, K_i, and K_d. The following segments provide a brief description and methodology for each algorithm.

Self-adaptive Differential Evolution (SaDE) is one of the popular variant of basic Differential Evolution (DE). DE is a population-based search algorithm that has shown to be helpful in solving optimization challenges. In DE, a randomly generated population is created at first, with each individual representing a potential solution. Mutation, crossover, and selection are all applied to the resultant population. The process is repeated until one or more termination criteria are met [50]. While basic DE employs the pre-specified values for control parameters scaling factor (F) and crossover factor (C_r), SaDE self-adjust these in each generation. When tested for the same benchmark problems, SaDE outperforms standard DE in many cases [51], hence it was chosen for

optimization purposes here. A relatable procedure to apply DE for an optimization problem is given below:

Self-Adaptive Differential Evolution (SaDE)

Start
Define the Objective function *Minimize* $[F_{ITAE}]$ (equation (37))
Set the parameters of SaDE as:
Population size $(N_p) = 50$
Maximum number of generations $(max_{gen}) = 1000$
Start generation count, $g = 0$
Generate initial population having n population vectors
for $i = 1$ to n, and $j = 1$ to number of variables

$$Z_{ij}^{g} = LB\,(j) + [UB\,(j) - LB\,(j)] * rand(0, 1)$$

Set initial scaling factor $(F_i^g) = 0.6$ and crossover factor $(C_{ri}^g) = 0.85$
while $g < max_{gen}$
Perform mutation as:
choose three random and distinct population vectors $r_1, r_2, r_3 \in [1, n]$
for each target vector Z_{ij}^g generate a mutant vector $V_{i,j}^g$ as

$$V_{i,j}^{g} = Z_{i,r_1}^{g} + F_i^{g}\left(Z_{i,r_2}^{g} - Z_{i,r_3}^{g}\right)$$

Perform crossover to generate trail vectors as:

$$U_{i,j}^{g} = \begin{cases} V_{i,j}^{g} & if\ rand_{i,j} \le C_{ri}^{g} \\ Z_{i,j}^{g} & otherwise \end{cases}$$

Execute selection of vectors for next generation as:

$$Z_{i,j}^{g+1} = \begin{cases} U_{i,j}^{g} & if\ f(U_{i,j}^{g}) \le f(Z_{i,j}^{g}) \\ Z_{i,j}^{g} & otherwise \end{cases}$$

Update F and C_r as follows (**peculiarity in SaDE**)

$$F_i^{g+1} = \begin{cases} F_l + rand_1 * F_u & if\ rand_2 \le 0.1 \\ F_i^{g} & otherwise \end{cases}$$

$$C_{ri}^{g+1} = \begin{cases} rand_3 & if\ rand_4 \le 0.1 \\ C_{ri}^{g} & otherwise \end{cases}$$

where, *rand* represent random number between 0 and 1, $F_l = 0.1$, and $F_u = 0.9$
end while
return the best solution, Z_{best}
Stop

Abdollahzadeh et al. [52] introduced AVOA, which is derived by studying the lifestyle of African vultures and how they collectively work to find food. Initially, a population of vultures is constructed to represent the feasible solutions in the search space. Each vulture's fitness is assessed in order to establish the best and second-best vultures. In addition, the remaining vultures are split into two groups, each of which represents a population that changes or replaces one of the two best vultures in each iteration [53]. The following is a detailed description of the process used by AVOA to solve the current optimization problem:

African Vultures Optimization Algorithm (AVOA)

Start
Define Objective function: *Minimize* $[F_{ITAE}]$ (equation (37))
Set AVOA parameters:

- Population size $(N) = 50$
- Maximum number of iterations (T_{max}) = 100*no. of variables
- $L_1 = 0.8$ and $L_2 = 0.2$
- $\omega = 2.5$
- *rand* = random value between 0 and 1, generated in each iteration
- $P_1, P_1, P_1 = 0.6, 0.4, 0.6$

Initialize the random population of vultures P_i ($i = 1$ to N, $j = 1$ to number of variables)
While iteration count $< T_{max}$
Evaluate fitness value for each vulture i.e. estimate F_{ITAE}
Set P_{BV1} value as the location of first best vulture and P_{BV2} as the second best vulture.
for each vulture P_i
select best vulture: $R_i = \begin{cases} P_{BV1} & if\ p_i = L_1 \\ P_{BV2} & if\ p_i = L_2 \end{cases}$ where $p_i = \frac{F_i}{\sum_{i=1}^{N} F_i}$
update $t = h \times \left(sin^{\omega}\left(\frac{\pi}{2}\frac{T_i}{T_{max}}\right) + cos\left(\frac{\pi}{2}\frac{T_i}{T_{max}}\right) - 1\right)$ where $h = -2$ to 2
and calculate $F = (2 \times rand_1 + 1) \times z \times \left(1 - \frac{T_i}{T_{max}}\right) + t$
if $|F| \ge 1$ and **if** $P_1 \ge rand_{p1}$
then $P_{i+1} = (R_i - D_i) \times F$ where $D_i = |X \times R_i - P_i|$, $X = 2 \times rand$
else $P_{i+1} = R_i - F + rand_2 \times ((UB - LB) \times rand_3 + LB)$
end
if $0.5 \le |F| < 1$ **then**
if $P_2 \ge rand_{p2}$
then $P_{i+1} = D_i \times (F + rand_4) - d(t)$ where $d\,(t) = R_i - P_i$
else $P_{i+1} = R_i - \left[\left(R_i \times \left(\frac{rand_5 \times P_i}{2\pi}\right) \times \cos\,(P_i)\right) + \left(R_i \times \left(\frac{rand_6 \times P_i}{2\pi}\right) \times \sin\,(P_i)\right)\right]$
end
else if $P_3 \ge rand_{p3}$
then $P_{i+1} = \left[\left(P_{BV1i} - \frac{P_{BV1i} \times P_i}{P_{BV1i} - P_i^2} \times F\right) + \left(P_{BV2i} - \frac{P_{BV2i} \times P_i}{P_{BV2i} - P_i^2} \times F\right)\right]/2$
else $P_{i+1} = R_i - |d\,(t)| \times F \times LF(x)$
end
end while
Return final P_{BV} and corresponding value of F_{ITAE}
Stop

VIII. CONTROLLER ANALYSIS

A. CONTROLLER GAINS

To find the best values for K_p, K_i, and K_d such that F_{ITAE} (equation (37)) is minimized, each of the aforementioned

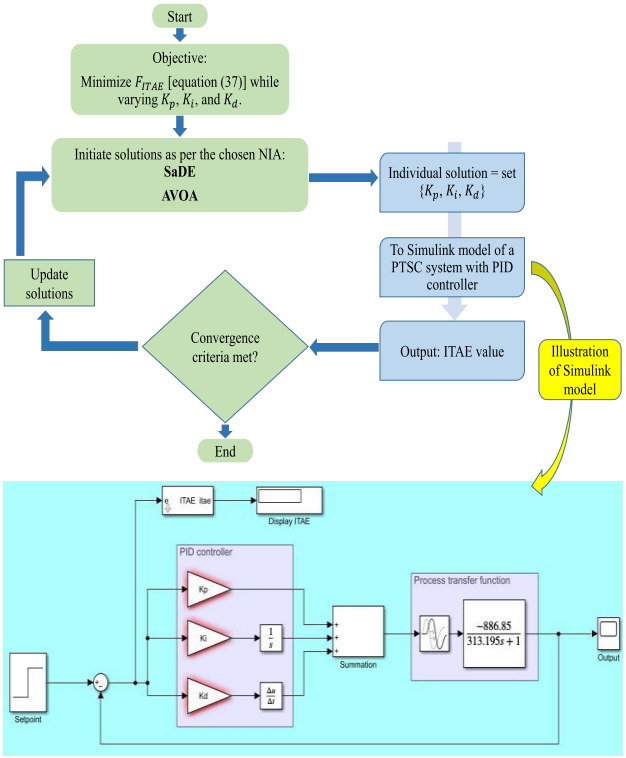

FIGURE 5. Optimization procedure along with the Simulink model of the designed controller.

TABLE 3. Values of K_p, K_i, and K_d after optimization.

Tuning method	Optimal values of gains for PID controller		
	K_p	K_i	K_d
SaDE-PID tuned	−0.001748	-8.9692×10^{-6}	−0.02179
AVOA-PID tuned	−0.00104	-7.5699×10^{-6}	−0.0977

techniques has been used one at a time. It is a prerequisite to provide the upper bound and lower bound of search spaces for SaDE and AVOA to start searching for best solution. Also, it is known that K_p, K_i, and K_d can take any value depending on the system. Therefore, initially the designed controller was tested for different random values, both positive as well negative. After, few trial and error runs the range of -2 to 2 was fixed for each of the PID gains.

As previously discussed, the controller is designed for LS-2 collector tested by SNL. Controller is aimed to control the HTF outlet temperature with HTF flowrate as manipulated variable. Set point is 173.30 °C and transfer function is derived as equation (34). Optimization procedure discussed in Figure 5 is followed for SaDE and AVOA with the mentioned range of PID gains. After optimization, the values obtained for K_p, K_i, and K_d are summarized in Table 3.

It is observed that values of K_p, K_i, and K_d predicted by SaDE gives less $ITAE = 5.724 \times 10^6$ compared to

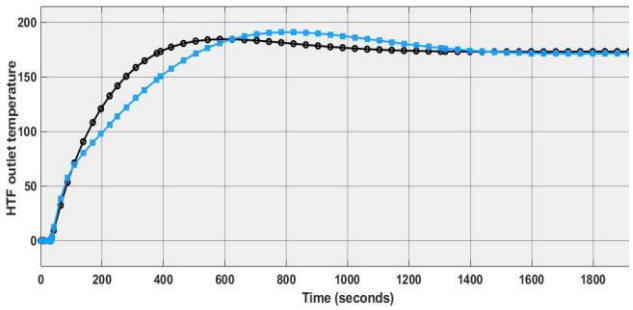

FIGURE 6. Step responses for the SaDE-PID tuned controller and AVOA-PID tuned controller.

TABLE 4. Transient response characteristics of the step responses in FIGURE 6.

Characteristic	Tuning method	
	SaDE-PID tuned	AVOA-PID tuned
Maximum overshoot (M_p)	6.5%	10.13%
Settling time (s_t)	798.74 sec.	1108.26 sec.
Rise time (r_t)	248.65 sec.	370.30 sec.
Delay time (d_t)	129.69 sec.	158.31 sec.

$ITAE = 1.306 \times 10^7$ for the values suggested by AVOA. Thus, for the given PTSC system under the mentioned operating conditions, SaDE provides better tuning of PID controller. It implies that comparable or better results can be obtained by employing different NIAs to solve the tuning optimization problem.

B. TRANSIENT RESPONSE CHARACTERISTICS

Despite the lower value of $ITAE$, there are other factors as well that characterize the proficiency of the controller. Generally, the transient response of the system with step input or simply step response is used to determine such factors. Thus, to further analyse the performance of the designed controller, the step responses of the SaDE-PID tuned and AVOA-PID tuned controller are plotted and shown in Figure 6.

Various transient response characteristics (maximum overshoot, settling time, rise time, and delay time) are estimated using the step responses shown in Figure 6 and are displayed in Table 4. Each of these characteristics have their own significance w.r.t. to the controller performance and thus becomes critical to analyse. It can be assessed from Table 4 that SaDE-PID tuned controller outperforms AVOA-PID tuned controller in terms of all the characteristics.

C. PERFORMANCE INDEXES

A criterion that relates each response to a single number, or a figure of merit, is ideal for comparing responses that use various sets of controller parameters. Such criteria use a certain way to keep score of the merit of controller and a lower score means a good controller. In control system design, these criteria are designated as performance indexes. One of these indexes represented as $ITAE$ is discussed in Section 4.3 to create an objective function for optimal tuning

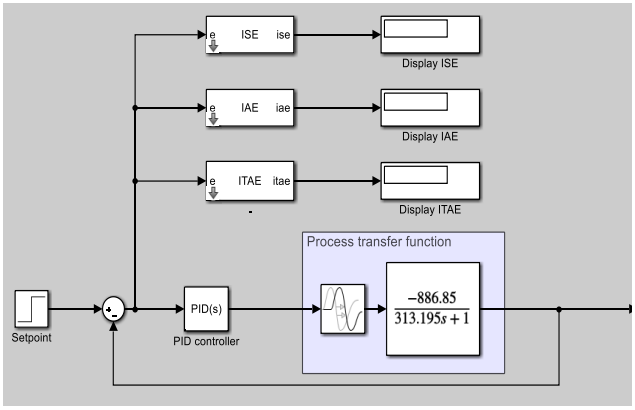

FIGURE 7. Picture of Simulink model to compare various performance indexes.

TABLE 5. Comparison on performance.

Performance index	Tuning method	
	SaDE-PID tuned	AVOA-PID tuned
ISE	2.361×10^6	2.793×10^6
IAE	2.779×10^4	3.867×10^4
ITAE	5.724×10^6	1.306×10^7

problem. Designed controller is already examined on this performance index but to check its reliability it is examined on the other indexes as well. A Simulink model shown in Figure 7 is developed and used to check the proficiency of designed controller over the different performance indexes.

The tuning parameters predicted by SaDE and AVOA are fed to the controller and the values of various performance indexes namely, Integral of the square of the error (ISE), Integral of the absolute value of error (IAE), and ITAE are noted. Table 5 compares the values of different performance indexes.

ISE values are comparable for both SaDE-PID tuned and AVOA-PID tuned controller. IAE value is relatively better for SaDE-PID tuned controller in comparison to AVOA-PID tuned controller. Interestingly, only in terms of ITAE, SaDE-PID tuned controller clearly outperforms the AVOA-PID tuned controller. Thus, it can be said that to check the dependability and robustness of a controller it is important to analyse its performance on more than one performance indexes.

IX. CONCLUSION

A detailed study confined to the dynamic modeling and control of single PTSC module has been presented here. Such a study could offer the foundation for being extended to different PTSC module types that are readily available globally and could be beneficial for increased solar energy utilization. An analytical dynamic model of PTSC is formulated by considering the energy balances across the HCE surfaces. An approach to determine the transfer function for a PTSC control system has been clearly outlined. A generic equation has been obtained that can relate the output of PTSC (outlet HTF temperature) with other variables like HTF flow rate, solar irradiation, and others.

The approach proposed for the development of transfer function is applied to a PTSC module tested by Sandia National Laboratories (SNL), USA. The transfer function relating the outlet HTF temperature with HTF flow rate is obtained. A controller is designed for PTSC such that a specific output temperature can be maintained by varying the HTF flowrate. Minimization of integral of time-weighted absolute error (ITAE) is utilized as an objective function to tune the controller for PTSC.

Tuning a PID controller is a complex problem and is resolved using suitable nature inspired algorithms (NIAs). In this line following deductions were made:

- A Simulink model is created to compute the resultant ITAE for given values of K_p, K_i, and K_d.
- We have demonstrated how NIAs can be used with ease to solve the formulated tuning optimization problem.
- Designed controller is tuned using Self-adaptive Differential Evolution (SaDE) and African Vultures Optimization Algorithm (AVOA).
- It was observed that values of K_p, K_i, and K_d predicted by SaDE gives less $ITAE = 5.724 \times 10^6$ compared to $ITAE = 1.306 \times 10^7$ for the values suggested by AVOA. Thus, for the given PTSC system under the mentioned operating conditions, SaDE provides better tuning of a PID controller.

Furthermore, to verify the reliability of the designed controller, it has been tested for various criteria and following inferences made:

- SaDE-PID tuned controllers outperform AVOA-PID tuned controller in terms of all other transient characteristics. It suggests that tuning optimization problem is dependent on the choice of NIA and hence, improved solution using other NIAs may be explored in future.
- When compared based on performance indexes, ISE values were comparable for both SaDE-PID tuned and AVOA-PID tuned controller. IAE value was relatively better and in terms of ITAE, SaDE-PID tuned controller clearly outperformed the AVOA-PID tuned controller. It is concluded that it's crucial to examine a controller's performance across a variety of performance indices to determine its dependability and robustness.

Industries like beverage industry, dairy industry, food industry and others require constant temperatures for certain processes, if temperatures are allowed to vary too much, they can harm both the finished product and the production processes. Thus, temperature control is crucial and if PTSCs are used to serve such processes then the controller designed and discussed here could be a useful asset for such integrations.

REFERENCES

[1] A. Goel, O. P. Verma, and G. Manik, "Analytical modeling of parabolic trough solar collector," in *Soft Computing: Theories and Applications*, vol. 425, R. Kumar, C. W. Ahn, T. K. Sharma, O. P. Verma, and A. Agarwal, Eds. Singapore: Springer, 2022, pp. 367–378, doi: 10.1007/978-981-19-0707-4_34.

[2] A. Goel and G. Manik, "Solar thermal system—An insight into parabolic trough solar collector and its modeling," in *Renewable Energy Systems*, A. T. Azar and N. A. Kamal, Eds. Cambridge, MA, USA: Academic, 2021, pp. 309–337, doi: 10.1016/B978-0-12-820004-9.00021-8.

[3] A. Goel, G. Manik, and R. Mahadeva, "A review of parabolic trough collector and its modeling," in *Advances in Intelligent Systems and Computing*, vol. 1053, M. Pant, T. Sharma, O. Verma, R. Singla, and A. Sikander, Eds. Singapore: Springer, 2020, pp. 803–813, doi: 10.1007/978-981-15-0751-9_73.

[4] E. F. Camacho and M. Berenguel, "Control of solar energy systems," *IFAC Proc. Volumes*, vol. 45, no. 15, pp. 848–855, 2012, doi: 10.3182/20120710-4-SG-2026.00181.

[5] E. F. Camacho, F. R. Rubio, M. Berenguel, and L. Valenzuela, "A survey on control schemes for distributed solar collector fields—Part I: Modeling and basic control approaches," *Sol. Energy*, vol. 81, no. 10, pp. 1240–1251, Oct. 2007, doi: 10.1016/j.solener.2007.01.002.

[6] O. P. Verma, G. Manik, and V. K. Jain, "Simulation and control of a complex nonlinear dynamic behavior of multi-stage evaporator using PID and fuzzy-PID controllers," *J. Comput. Sci.*, vol. 25, pp. 238–251, Mar. 2018, doi: 10.1016/j.jocs.2017.04.001.

[7] X. H. Gao, S. Wei, and Z. G. Su, "Optimal model predictive rejection control for nonlinear parabolic trough collector with lumped disturbances," *Trans. Inst. Meas. Control*, vol. 43, no. 9, pp. 1903–1914, Jun. 2021, doi: 10.1177/0142331220983651.

[8] A. Desideri, R. Dickes, J. Bonilla, L. Valenzuela, S. Quoilin, and V. Lemort, "Steady-state and dynamic validation of a parabolic trough collector model using the ThermoCycle Modelica library," *Sol. Energy*, vol. 174, pp. 866–877, Nov. 2018, doi: 10.1016/j.solener.2018.08.026.

[9] M. Eck and T. Hirsch, "Dynamics and control of parabolic trough collector loops with direct steam generation," *Sol. Energy*, vol. 81, no. 2, pp. 268–279, Feb. 2007, doi: 10.1016/j.solener.2006.01.008.

[10] T. Stuetzle, N. Blair, J. W. Mitchell, and W. A. Beckman, "Automatic control of a 30 MWe SEGS VI parabolic trough plant," *Sol. Energy*, vol. 76, nos. 1–3, pp. 187–193, Jan. 2004, doi: 10.1016/j.solener.2003.01.002.

[11] S. Guo, D. Liu, X. Chen, Y. Chu, C. Xu, Q. Liu, and L. Zhou, "Model and control scheme for recirculation mode direct steam generation parabolic trough solar power plants," *Appl. Energy*, vol. 202, pp. 700–714, Sep. 2017, doi: 10.1016/j.apenergy.2017.05.127.

[12] P. Naidoo and T. I. Van Niekerk, "Optimising position control of a solar parabolic trough," *South Afr. J. Sci.*, vol. 107, nos. 3–4, pp. 2–7, Mar. 2011, doi: 10.4102/sajs.v107i3/4.452.

[13] A. Palacios, D. Amaya, O. Ramos, A. Palacios, D. Amaya, and O. Ramos, "Solar tracking control of a parabolic trough collector by traditional PID, fuzzy sets and particle swarm optimization algorithm," *Int. Rev. Autom. Control (IREACO)*, vol. 14, no. 3, pp. 124–134, May 2021, doi: 10.15866/IREACO.V14I3.19267.

[14] M. Gálvez-Carrillo, R. D. Keyser, and C. Ionescu, "Nonlinear predictive control with dead-time compensator: Application to a solar power plant," *Sol. Energy*, vol. 83, no. 5, pp. 743–752, May 2009, doi: 10.1016/J.SOLENER.2008.11.005.

[15] S. J. Navas, F. R. Rubio, and P. Ollero, "Optimum control of parabolic trough solar fields with partial radiation," *IFAC-PapersOnLine*, vol. 50, no. 1, pp. 109–114, Jul. 2017, doi: 10.1016/j.ifacol.2017.08.019.

[16] W. A. K. Al-Maliki, F. Alobaid, V. Kez, and B. Epple, "Modelling and dynamic simulation of a parabolic trough power plant," *J. Process Control*, vol. 39, pp. 123–138, Mar. 2016, doi: 10.1016/j.jprocont.2016.01.002.

[17] C. A. Mosbah, M. Tadjine, M. Chakir, and M. S. Boucherit, "On the control of parabolic solar collector: The zipper approach," *Int. J. Renew. Energy Res.*, vol. 6, no. 3, pp. 1100–1108, 2016, doi: 10.20508/ijrer.v6i3.4225.g6893.

[18] J. M. Escaño, A. J. Gallego, A. J. Sánchez, L. J. Yebra, and E. F. Camacho, "Nonlinear fuzzy model predictive control of the TCP-100 parabolic trough plant," in *Proc. Atlantis Stud. Uncertainty Model.*, 2021, pp. 235–241, doi: 10.2991/asum.k.210827.032.

[19] S. Elmetennani and T. M. Laleg-Kirati, "Fuzzy universal model approximator for distributed solar collector field control," in *Proc. UKACC Int. Conf. Control (CONTROL)*, Jul. 2014, pp. 203–208, doi: 10.1109/CONTROL.2014.6915140.

[20] A. J. Gallego and E. F. Camacho, "Adaptative state-space model predictive control of a parabolic-trough field," *Control Eng. Pract.*, vol. 20, no. 9, pp. 904–911, Sep. 2012, doi: 10.1016/j.conengprac.2012.05.010.

[21] V. E. Dudley, G. J. Kolb, M. Sloan, and D. Kearney, *Test Results–SEGS LS2 Collector*. Albuquerque, NM, USA: Sandia National Laboratories, 1994.

[22] F. Incropera and D. Dewitt, *Fundamentals of Heat and Mass Transfer*, 6th ed. Hoboken, NJ, USA: Wiley, 2006.

[23] V. Gnielinski, "On heat transfer in tubes," *Int. J. Heat Mass Transf.*, vol. 63, pp. 134–140, Aug. 2013, doi: 10.1016/j.ijheatmasstransfer.2013.04.015.

[24] A. Goel, G. Manik, and O. P. Verma, "Combinatorial and geometric optimization of a parabolic trough solar collector," *Korean J. Chem. Eng.*, vol. 38, no. 2, pp. 1–22, 2021, doi: 10.1007/s11814-021-0939-5.

[25] S. A. Kalogirou, *Solar Energy Engineering: Processes and Systems*, 2nd ed. Cambridge, MA, USA: Academic, 2013, doi: 10.1016/b978-0-12-374501-9.00014-5.

[26] A. C. Ratzel, C. E. Hickox, and D. K. Gartling, "Techniques for reducing thermal conduction and natural convection heat losses in annular receiver geometries," *J. Heat Transf.*, vol. 101, no. 1, pp. 108–113, Feb. 1979, doi: 10.1115/1.3450899.

[27] A. Goel and G. Manik, "Step towards sustainability: Techno-economic optimization of a parabolic trough solar collector using multi-objective genetic algorithm," *Thermal Sci. Eng. Prog.*, vol. 37, Jan. 2023, Art. no. 101539, doi: 10.1016/J.TSEP.2022.101539.

[28] S. W. Churchill and R. Usagi, "A general expression for the correlation of rates of transfer and other phenomena," *AIChE J.*, vol. 18, no. 6, pp. 1121–1128, Nov. 1972, doi: 10.1002/aic.690180606.

[29] W. M. Rohsenow and J. R. Hartnett, *Handbook of Heat Transfer*, 3rd ed. New York, NY, USA: McGraw-Hill, 1999.

[30] V. T. Morgan, "The overall convective heat transfer from smooth circular cylinders," *Adv. Heat Transf.*, vol. 11, pp. 199–264, Jan. 1975, doi: 10.1016/S0065-2717(08)70075-3.

[31] H. Yılmaz and M. S. Söylemez, "Thermo-mathematical modeling of parabolic trough collector," *Energy Convers. Manage.*, vol. 88, pp. 768–784, Dec. 2014, doi: 10.1016/j.enconman.2014.09.031.

[32] F. Lippke, "Simulation of the part-load behaviour of a 30 MW SEGS plant," Sandia Nat. Lab., Albuquerque, NM, USA, Tech. Rep. SAND-95-1293, 1995.

[33] J. D. Álvarez, L. J. Yebra, and M. Berenguel, "Repetitive control of tubular heat exchangers," *J. Process Control*, vol. 17, no. 9, pp. 689–701, Oct. 2007, doi: 10.1016/J.JPROCONT.2007.02.003.

[34] J. D. Álvarez, L. J. Yebra, and M. Berenguel, "Adaptive repetitive control for resonance cancellation of a distributed solar collector field," *Int. J. Adapt. Control Signal Process.*, vol. 23, no. 4, pp. 331–352, Apr. 2009, doi: 10.1002/ACS.1045.

[35] E. F. Camacho, M. Berenguel, F. R. Rubio, and D. Martínez, "Basic control of parabolic troughs," in *Control of Solar Energy Systems* (Advances in Industrial Control). London, U.K.: Springer, 2012, doi: 10.1007/978-0-85729-916-1_4.

[36] E. F. Camacho, M. Berenguel, F. R. Rubio, and D. Martínez, "Advanced control of parabolic troughs," in *Control of Solar Energy Systems Advances in Industrial Control*. London, U.K.: Springer, 2012, doi: 10.1007/978-0-85729-916-1_5.

[37] C. M. Cirre, M. Berenguel, L. Valenzuela, and E. F. Camacho, "Feedback linearization control for a distributed solar collector field," *Control Eng. Pract.*, vol. 15, no. 12, pp. 1533–1544, Dec. 2007, doi: 10.1016/J.CONENGPRAC.2007.03.002.

[38] S. Koch, M. Eck, and T. Hirsch, "Modelling and control of a solar-thermal parabolic trough DSG superheater with several parallel rows and central steam separation," in *Proc. Energy Sustainability Conf.*, 2009, pp. 1005–1014, doi: 10.1115/ES2007-36162.

[39] A. Goel, G. Manik, and O. P. Verma, "Designing a robust analytical model of a parabolic trough solar collector through in-depth analysis of convective heat transfers," *Arabian J. Sci. Eng.*, vol. 47, no. 5, pp. 6535–6557, May 2022, doi: 10.1007/s13369-021-06473-y.

[40] J. J. Gude, E. Kahoraho, and J. Etxaniz, "Practical aspects of PID controllers: An industrial experience," in *Proc. IEEE Conf. Emerg. Technol. Factory Autom.*, Sep. 2006, pp. 870–878, doi: 10.1109/ETFA.2006.355215.

[41] W. Zhang, Y. Cui, X. Ding, Z. Yin, and Y. Wang, "A novel tuning method of differential forward robust PID controller for integrating systems plus time delay based on direct synthesis method," *Int. J. Syst. Sci.*, vol. 52, no. 2, pp. 238–262, Jan. 2021, doi: 10.1080/00207721.2020.1825871.

[42] M. Mahmoodabadi, M. Taherkhorsandi, M. Talebipour, and K. Castillo-Villar, "Adaptive robust PID control subject to supervisory decoupled sliding mode control based upon genetic algorithm optimization," *Trans. Inst. Meas. Control*, vol. 37, no. 4, pp. 505–514, Aug. 2015, doi: 10.1177/0142331214543295.

[43] K. Ogata, *Modern Control Engineering*, 5th ed. Upper Saddle River, NJ, USA: Prentice-Hall, 2010.

[44] D. R. Coughanowr and S. E. LeBlanc, *Process Systems Analysis and Control*. New York, NY, USA: McGraw-Hill, 2009, p. 630.
[45] J. Pongfai, C. Angeli, P. Shi, X. Su, and W. Assawinchaichote, "Optimal PID controller autotuning design for MIMO nonlinear systems based on the adaptive SLP algorithm," *Int. J. Control, Autom. Syst.*, vol. 19, no. 1, pp. 392–403, Jan. 2021, doi: 10.1007/s12555-019-0680-6.
[46] R.-E. Precup, R.-C. David, R.-C. Roman, A.-I. Szedlak-Stinean, and E. M. Petriu, "Optimal tuning of interval type-2 fuzzy controllers for nonlinear servo systems using slime mould algorithm," *Int. J. Syst. Sci.*, pp. 1–16, Jun. 2021, doi: 10.1080/00207721.2021.1927236.
[47] S. B. Joseph, E. G. Dada, A. Abidemi, D. O. Oyewola, and B. M. Khammas, "Metaheuristic algorithms for PID controller parameters tuning: Review, approaches and open problems," *Heliyon*, vol. 8, no. 5, May 2022, Art. no. e09399, doi: 10.1016/J.HELIYON.2022.E09399.
[48] R. L. L. Guong, S. B. Hisham, I. Elamvazuthi, S. Aole, S. Parasuraman, and M. K. A. A. Khan, "PID tuning of process plant using particle swarm optimization," in *Proc. IEEE 4th Int. Symp. Robot. Manuf. Autom. (ROMA)*, Dec. 2018, pp. 1–6, doi: 10.1109/ROMA46407.2018.8986712.
[49] A. Y. Jaen-Cuellar, R. de J. Romero-Troncoso, L. Morales-Velazquez, and R. A. Osornio-Rios, "PID-controller tuning optimization with genetic algorithms in servo systems," *Int. J. Adv. Robotic Syst.*, vol. 10, no. 9, p. 324, Sep. 2013, doi: 10.5772/56697.
[50] M. Pant, H. Zaheer, L. Garcia-Hernandez, and A. Abraham, "Differential evolution: A review of more than two decades of research," *Eng. Appl. Artif. Intell.*, vol. 90, Apr. 2020, Art. no. 103479, doi: 10.1016/j.engappai.2020.103479.
[51] S. K. Goudos, K. B. Baltzis, K. Antoniadis, Z. D. Zaharis, and C. S. Hilas, "A comparative study of common and self-adaptive differential evolution strategies on numerical benchmark problems," *Proc. Comput. Sci.*, vol. 3, pp. 83–88, Jan. 2011, doi: 10.1016/J.PROCS.2010.12.015.
[52] B. Abdollahzadeh, F. S. Gharehchopogh, and S. Mirjalili, "African vultures optimization algorithm: A new nature-inspired metaheuristic algorithm for global optimization problems," *Comput. Ind. Eng.*, vol. 158, Aug. 2021, Art. no. 107408, doi: 10.1016/J.CIE.2021.107408.
[53] A. Goel, R. Mahadeva, and G. Manik, "Analysis and optimization of parabolic trough solar collector to improve its optical performance," *J. Sol. Energy Eng.*, vol. 145, no. 3, Jun. 2023, Art. no. 031009, doi: 10.1115/1.4055995.

ANUBHAV GOEL received the B.Tech. degree in electrical and electronics engineering from Uttar Pradesh Technical University (UPTU), Lucknow, Uttar Pradesh, India, in 2009, the M.Tech. degree in instrumentation and control from Maharishi Dayanand University (MDU), Rohtak, Haryana, India, in 2016, and the Ph.D. degree from the Indian Institute of Technology (IIT) Roorkee, Uttarakhand, India, in 2023. From 2009 to 2014 and from January 2017 to December 2017, he was with different engineering institutes in INDIA and in different positions. His research interests include modeling, simulation, optimization, and control of parabolic trough solar collector for industrial process heating applications.

RAJESH MAHADEVA (Member, IEEE) received the B.E. degree in electronics and instrumentation engineering from the Samrat Ashok Technological Institute (SATI), Vidisha, Madhya Pradesh, India, in 2006, the M.Tech. degree in control and instrumentation engineering from the National Institute of Technology (NIT), Jalandhar, Punjab, India, in 2009, and the Ph.D. degree from the Department of Polymer and Process Engineering, Indian Institute of Technology (IIT) Roorkee, Uttarakhand, India, in 2022. From 2011 to 2017, he was an Assistant Professor with the Technocrats Institute of Technology (TIT), Bhopal, and Marwadi University (MU), Rajkot, India. He is currently a Researcher with the Department of Physics, Khalifa University of Science and Technology, Abu Dhabi, UAE. His research interests include modeling, simulation, optimization, and control of desalination and water treatment plants/processes using artificial intelligence techniques.

SHASHIKANT P. PATOLE (Member, IEEE) received the B.Sc., M.Sc., and M.Phil. degrees in physics from the University of Pune (UoP), India, and the Ph.D. degree in nano science and technology from Sungkyunkwan University (SKKU), Suwon, South Korea, in 2010. Since 2017, he has been an Assistant Professor with the Physics Department, Khalifa University of Science and Technology (KU), Abu Dhabi, UAE. Before joining KU, he was an Entrepreneur and a Postdoctoral Researcher with the King Abdulla University of Science and Technology (KAUST), Saudi Arabia. In KAUST, he served as a Founding Member of the Laboratory for Carbon Nanostructures and the Co-Founder of Graphene Crystal startup company. He has published more than 50 articles. His research interests include the development and commercialization of advanced quantum materials for sustainable energy and environment, carbon nanotubes, graphene, and other 2-D materials in membrane technology, structural composites and energy, optoelectronics, electron field emission, and photovoltaic, and aberration-corrected transmission electron microscopy.

GAURAV MANIK received the B.Tech. degree in chemical engineering from HBTI Kanpur, the M.Tech. degree in chemical engineering from IIT Kanpur, and the Ph.D. degree in chemical engineering from IIT Bombay. He joined the Department of Polymer and Process Engineering, IIT Roorkee, in January 2013, as an Assistant Professor, where he is currently serving as an Associate Professor and the Head. Prior to joining IITR, he has served extensively in the industry (3M, Indo Gulf Fertilizers & Chemicals Ltd., and Classic Stripes Pvt., Ltd.) and academia (BITS Pilani and BIET Jhansi) totaling up his rich experience to more than 18 years. In industry, he is credited with creating and commercializing several innovative products and protecting IP through a significant number of patents and a record of inventions. He has more than 150 research publications in international peer-reviewed SCI journals, patent applications, conferences, and book chapters. He has significantly valued 74 publications in peer-reviewed chemical engineering, biomedical engineering, and polymer science and engineering journals of repute, such as *Renewable and Sustainable Energy Reviews*, *Energy*, *Microchimica Acta*, *Composites—B: Engineering*, *Applied Surface Science*, *Polymer*, *Progress in Organic Coatings*, and *ACS Applied Materials and Interfaces*, to name a few, and holds seven granted patents/patent applications of industrial commercial relevance, and has contributed to 22 books and 49 conference publications. He has executed/supervised five research projects and supervised projects of one postdoctoral candidate, seven Ph.D. students (more than three ongoing), 11 M.Tech. students, and 25 B.Tech. students. At IIT Roorkee, he has recorded the highest average number of research journal publications/patent applications consistently in the last few years and maintained the highest student appraisal score in teaching. His research interests include molecular modeling and simulations of polymers/materials, biosensing, chemical process modeling and simulation, and the development of novel and industrially significant sustainable polymer composites, coatings, sealants, quantum dots, and adhesives. Among several awards received to disseminate professional knowledge and research, he has been awarded the prestigious APAC level TechForum Contribution Award at 3M, in 2012, the Best Innovative Product Design Award twice at 3M, in 2010 and 2011, the Secondment as a Visiting Faculty sanctioned by the President of India for teaching at the international platform at the Asian Institute of Technology, Thailand, and the VICAL Award for Best Technical Paper by Institute of Chemical Engineers (IIChe), India. He has been an invited speaker, guest, and session chair at several national and international conferences and workshops in India and abroad and serves on the Board of Directors for the STEM Research Society, India.